Regulation of IGF - mTOR signalling by miRNA in childhood adrenocortical tumors

Mabrouka Doghman[1,2,*], **Abeer EL Wakil**[1,2,*], **Bruno Cardinaud**[1,2,+], **Emilie Thomas**[3], **Jinling Wang**[4], **Wei Zhao**[5], **Maria Helena C. Peralta-Del Valle**[6], **Bonald C. Figueiredo**[6], **Gerard P. Zambetti**[4], and **Enzo Lalli**[1,2]

[1] Institut de Pharmacologie Moléculaire et Cellulaire CNRS UMR 6097

[2] Université de Nice - Sophia Antipolis, Valbonne, France

[3] Programme Carte d'Identité des Tumeurs, Ligue Nationale Contre Le Cancer, Paris, France

[4] Department of Biochemistry, St. Jude Children's Research Hospital, Memphis TN, USA

[5] Department of Biostatistics, St. Jude Children's Research Hospital, Memphis TN, USA

[6] Instituto de Pesquisa Pelé Pequeno Principe and Faculdades Pequeno Principe, Curitiba PR, Brazil

Abstract

MicroRNAs (miRNAs) act at the post-transcriptional level to control gene expression in virtually every biological process, including oncogenesis. Here we report the identification of a set of miRNAs that are differentially regulated in childhood adrenocortical tumors, including miR-99a and miR-100. Functional analysis of these miRNAs in adrenocortical tumor cell lines showed that they coordinately regulate expression of the IGF-mTOR-raptor signalling pathway through binding sites in their 3′ UTRs. In these cells, the active Ser2448-phosphorylated form of mTOR is present only in mitotic cells in association with the mitotic spindle and midbody in the G2/M phases of the cell cycle. Pharmacological inhibition of mTOR signalling by everolimus greatly reduces tumor cell growth in vitro and in vivo. Our results reveal a novel mechanism of regulation of mTOR signalling by miRNAs, and they lay the groundwork for clinical evaluation of mTOR pathway drugs for treatment of adrenocortical cancer.

Keywords

adrenal gland; cancer; miRNA; signaling

Introduction

Adrenocortical tumors (ACT) in children may occur sporadically or in association with other types of neoplasms in the context of multiple neoplasia syndromes linked to germline tumor suppressor gene mutations (1). The incidence of these tumors is highest during the first three years of life and is several times more frequent in southern Brazil than in the rest of the world

(2). In that geographical region, childhood ACT are almost invariably associated with the germline R337H tumor protein p53 (*TP53*) mutation (3). These tumors are believed to be derived from the fetal adrenal because of their age distribution, their pattern of hormone secretion and their molecular phenotype (2,4).

While the most common genetic basis of childhood ACT are germline *TP53* mutations with loss of heterozygosity (LOH) in the tumor, our knowledge of the molecular pathogenesis of these neoplasms is still limited. A very frequent feature is represented by LOH of the distal region of the short arm of chromosome 11, with preferential expression of the imprinted paternal allele and overexpression of the IGF2 growth factor (4,5). IGF2 signalling through the IGF-1R is thought to represent an important mechanism for ACT growth and a relevant therapeutic target (6,7). In addition, amplification and overexpression of the nuclear receptor Steroidogenic Factor-1 (SF-1; NR5A1) is thought to play an important role in ACT pathogenesis (8,9). Last, a study of protein-coding mRNAs found a distinct pattern of their expression in childhood ACT compared to normal adrenal cortex and also identified a set of transcripts whose expression is related to prognosis (10).

miRNAs belong to a class of small noncoding RNAs of ~21 nt length that control gene expression at the post-transcriptional level. In their mature form, miRNAs recognize by base-pairing sequences in the 3′UTR of protein-coding transcripts, leading to translational repression or mRNA degradation (11). miRNAs are involved in virtually every biological process, from development to viral infection, and are also associated with oncogenesis (12). In addition, a great number of known miRNAs are located at fragile sites and genomic regions implicated in cancer (13).

As part of our effort to elucidate the genetic determinants of childhood ACT, in this study we analyzed the miRNA expression pattern of childhood ACT. A group of miRNAs was found to be differentially expressed in ACT compared with normal adrenal. We focused our functional analysis on miR-99a and miR-100, which are significantly downregulated in ACT and share the same seed sequence. Among the predicted targets of these miRNAs, transcripts are found that encode key components of the IGF (IGF-1R) and mTOR (mTOR and raptor) signalling pathways. Here we show that mTOR signalling is activated in ACT and that miR-99a and miR-100 regulate expression of mTOR, raptor and IGF-1R in adrenocortical cancer cells. Moreover, the specific mTOR inhibitor RAD001 (everolimus) potently suppresses adrenocortical cancer cell proliferation *in vitro* and when grown as xenografts in immunodeficient mice. These data reveal a novel layer of regulation of IGF and mTOR signalling by miRNAs and show that mTOR inhibition represents a potential new therapeutic tool in adrenocortical cancer.

Materials and Methods

Human subjects

All patients and normal subjects gave their informed consent to this study, that was approved by the Ethical Committees of Pequeno Principe and St. Jude Children's Research Hospitals. Patients' clinical data are reported in Supplementary Table 1. Normal adrenal glands were obtained with IRB approval as discarded tissue from cases of Wilms' tumor. These patients, whose age ranged from 2 to 6 years, had not received chemotherapy before surgery. Normal adrenal cortex samples were isolated by an American Board–certified pathologist, snap-frozen in liquid nitrogen and processed for RNA extraction as described below.

miRNA expression studies

RNA was extracted from frozen tissue samples using the miRNeasy Mini Kit (Qiagen, Valencia, CA). 200 ng of total RNA from each sample was labelled and hybridized to human V2 microarrays (Agilent, Massy, France), following the manufacturer's procedures. The original expression data were first thresholded in such a way that any value less than the threshold was assigned to be equal to the threshold and any value above the threshold was left intact. The thresholded data were then log2 transformed and used for further analysis. We used Kruskal-Wallis test to compare the median expression levels between the normal and ACT samples in each probe set. The probe sets with p value less than 0.01 and signals present in at least 10 samples were used to make the heatmap plot. The threshold used in this study is 1. All analyses were implemented in R, version 2.6.2. Microarray data were deposited in the GEO database under record number GSE19856. Taqman RT-qPCR (Applied Biosystems, Foster City, CA) was used to confirm the expression levels of the miRNAs identified as differentially expressed by microarray plus the let-7a miRNA as a control. RNU48 was used as a reference gene for miRNA qPCR. For target gene identification, the Targetscan database (http://www.targetscan.org/) was interrogated.

Immunoblotting

Protein extracts were prepared by homogeneization of tissues and cells in Laemmli buffer (50 mM Tris-HCl, pH 6.8, 50% glycerol, 2% SDS, 0.02% bromophenol blue) containing 5% β-mercaptoethanol. Proteins were separated by SDS-PAGE and transferred to a nitrocellulose membrane (Schleicher & Schuell, Versailles, France). Primary antibodies used were anti mTOR (#2833 from Abcam, Paris, France), anti phospho-mTOR (Ser 2448) (#2971 from Cell Signaling Technology, Danvers, MA), anti raptor (#2280 from Cell Signaling Technology), anti rictor (#2114 from Cell Signaling Technology), anti IGF-1Rβ (#3027 from Cell Signaling Technology) and anti p42/p44 MAP kinases (#9102 from Cell Signaling Technology). Immunoblot was performed using a chemiluminescence system for protein detection (GE Healthcare, Orsay, France). Bands on blots were quantified using the ImageJ (http://rsbweb.nih.gov/ij/) software.

mTOR activity EIA assay

Tissue lysates were prepared by homogenization in lysis buffer (50 mM Tris-HCl pH 7.4, 100 mM NaCl, 50 mM β-glycerophosphate, 10% glycerol, 1% Tween-20, 1 mM EDTA, 20 nM microcystin-LR, 25 mM NaF) supplemented with protease inhibitor cocktail (Sigma-Aldrich, St. Quentin Fallavier, France). After centrifugation at $16000g$ for 20 minutes to eliminate debris, total protein concentration in the lysates was adjusted to 3 mg/mL and 0.8 mL of the lysates was incubated with anti mTOR-agarose beads (Abcam) for 2h at 4°C. The immunoprecipitates were then washed twice with lysis buffer and mTOR activity in the tissue lysates was measured with an immunoenzymatic assay (K-LISA mTOR activity kit; Calbiochem, Nottingham, UK) using a recombinant GST-p70S6K protein as a substrate, following the manufacturer's instructions.

Immunohistochemistry

It was performed on tumor paraffin sections after antigen retrieval using antibodies directed against phospho-mTOR (Ser 2448) (#2976 from Cell Signaling Technology) and phospho-RPS6 (Ser240/244) (#2215 from Cell Signaling Technology). Immunoreactivity was graded with scores from 0 to +++, which corresponded to negative, weak, intermediate, or strong staining intensity.

Transfections and luciferase assay

mTOR (nt 7782 – 8707 of sequence NM_004958), raptor (nt 4957 – 5361 of sequence NM_020761) and IGF-1R (nt 9543 – 9833 of sequence NM_000875) 3′ UTR sequences were PCR-amplified from a HeLa cell cDNA library (Clontech, Saint-Germain-en-Laye, France) using the primers shown in Supplementary Table 2 and cloned in the *NotI – XhoI* sites of the double luciferase psiCHECK-2 vector (Promega, Charbonnières-les-Bains, France) appended to the *Renilla* luciferase gene. Deletions in the 3′ UTR predicted miR99a/miR-100 binding sites were made by QuickChange mutagenesis (Stratagene, La Jolla, CA). HEK 293T cultured in DMEM (4.5 g/L glucose) supplemented with 10% FCS and antibiotics in 96-well white plates (Costar, Amsterdam, The Netherlands) were reverse-transfected in triplicate with 3′ UTR reporter constructs using Lipofectamine 2000 (Invitrogen, Cergy Pontoise, France) and pre-miR-99a, pre-miR-100 or negative control #1 precursor molecules (Ambion, Austin, TX). *Renilla* and firefly luciferase activities were measured with a Luminoskan Ascent (Thermo Labsystems, Courtaboeuf, France) luminometer. For each sample, *Renilla* luciferase activity was normalized by firefly luciferase activity. Each experiment was repeated three times in triplicate.

Adrenocortical tumor cell lines culture

H295R cells were cultured in DMEM/F12 supplemented with 2% NuSerum (Becton Dickinson, Le Pont de Claix, France), 1% ITS+ (Becton Dickinson) and antibiotics. SW-13 cells were cultured in DMEM/F12 medium supplemented with 10% FCS (Invitrogen) and antibiotics. HAC15 cells were cultured in DMEM/F12 supplemented with 10% cosmic calf serum (HyClone, Logan, UT), 1% ITS+ and antibiotics. Primary cells isolated from a pediatric ACT were cultured as described (14). As a method of authentication, the karyotype of cell lines and the steroid secretion profile of H295R cells were periodically tested.

miRNA knockdown

For endogenous miRNA knockdown, 1×10^5 cells/well were seeded in 12-well plates and transfected with miR-100 – specific or scramble control miRCURY LNA knockdown probes (Exiqon, Vedbaek, Denmark) using Lipofectamine 2000 (Invitrogen). 48 hours after transfection, levels of endogenous mTOR, raptor and IGF-1R were analyzed by Western blotting.

Immunofluorescence

It was performed on formaldehyde-fixed H295R cells cultured on glass slides using the anti mTOR (#2983 from Cell Signaling Technology), anti phospho-mTOR (Ser 2448) (#2976 from Cell Signaling Technology) and anti β-tubulin (Sigma-Aldrich) as primary antibodies revealed with Alexa594 - and Alexa488 - labelled secondary antibodies (Invitrogen). DAPI was used as nuclear counterstain. Images were acquired with a Zeiss Axioplan 2 fluorescence microscope coupled to a digital CCD camera and processed using ImageJ.

Xenografts

6×10^6 H295R cells were inoculated subcutaneously into the right flank of four-week old female NOD/SCID/γ_c^{null} mice. Three weeks later, when palpable tumors appeared, injected mice were randomly assigned to three groups of 8 animals treated with placebo or with a preparation of RAD001 for oral administration (3 and 10 mg/kg/day). Drugs were administered by gavage and tumor growth was monitored by measuring with a vernier caliper and calculating tumor volume (length × width × height × π/6). After the end of treatment, animals were euthanized according to the institutional animal care and use committee protocol. Xenografts were excised, weighted and either frozen in OCT or formaldehyde-fixed and included in paraffin for histological studies. Blood vessels were stained with Texas red – conjugated tomato lectin

(Vector, Burlingame, CA) and IHC for phospho-RPS6 was performed as described before (see Immunohistochemistry section).

Results

A set of miRNAs is differentially expressed in childhood ACT

We investigated miRNA expression in a series of 25 ACT (patients' clinical data are reported in Supplementary Table 1) and compared it with a group of 5 normal adrenocortical samples from age-matched subjects. Significant modulation of expression in ACT was found for 26 miRNAs with a *P* value <0.01. These miRNAs are shown in the heatmap in Figure 1. The majority (77%) of the differentially expressed miRNAs was downregulated in ACT compared to normal adrenal. Differentially regulated expression of all these miRNAs in ACT compared to normal adrenal cortex was confirmed by Taqman qPCR, while expression of the let-7a miRNA, which was not detected as differentially expressed in the microarray study, was not significantly different (Supplementary Figure 1).

ACT and normal samples were clustered into two distinct groups by unsupervised analysis, except for a single ACT sample whose miRNA expression profile clustered together with the normal group. Further analysis showed that inside the ACT cluster, two subclusters were present (T1, more distant from the normal group, and T2, closer to the normal group, see Figure 1). Probability of relapse was significantly associated with localization in the T1 subcluster (p=0.002, Fisher's exact test), while histological type (adenoma or carcinoma) was not significantly associated with any group of samples (p=0.35, Fisher's exact test). The expression of no single miRNA could perfectly discriminate cases with relapse from cases without relapse.

mTOR, raptor and IGF-1R, are overexpressed in ACT and upregulated by miR-100 knockdown in adrenocortical tumor cell lines

Among the most significantly downregulated miRNAs in ACT were miR-99a and miR-100, which share the same seed sequence and are predicted to target the 3′ UTRs of pivotal components of IGF (IGF1R) and mTOR [FRAP1 (mTOR) and RPTOR (raptor)] signaling (Supplementary Figure 2). While the importance of IGF signalling in ACT is well known (6, 7, 15), no data exist yet about the involvement of the mTOR pathway in the pathogenesis of ACT. We studied the expression of mTOR (and its active phosphorylated form at Ser2448), raptor and IGF-1R proteins in a series of ACT samples and compared it to normal adrenal cortex samples. mTOR, phospho-mTOR (Ser2448), raptor and IGF-1R protein levels were significantly higher in ACT (Figure 2A and Supplementary Figure 3). Conversely, the other mTOR-associated protein rictor was not detectable either in normal adrenal samples and in ACT (data not shown). mTOR activity was also significantly higher in ACT compared to normal adrenocortical tissue (Figure 2B). Finally, phosphorylation of mTOR at Ser2448 and of ribosomal protein S6 as markers of active mTOR signalling were detected in ACT by immunohistochemistry (Figure 2C). Quantification of IHC results is shown in Supplementary Table 3. Taken together, these results show that mTOR signalling is active in ACT. To investigate whether downregulation of endogenous miR-100 can modulate the levels of mTOR, raptor and IGF-1R proteins, we transfected a specific miR-100 knockdown probe or a control probe into two different human adrenocortical cell lines (H295R and SW-13) and detected a dose-dependent increase in mTOR, raptor and IGF-1R proteins expression only after miR-100 specific knockdown (Figure 2D).

miRNA of the miR-100 family regulate the expression of mTOR, raptor and IGF-1R through their 3′ UTRs

With the purpose to assess whether miR-99a and miR-100 can directly regulate the expression of mTOR, raptor and IGF-1R, we fused portions of the 3′ UTR sequences of these genes

harboring predicted binding sites for miR-99a/miR-100 to the luciferase reporter gene and performed transfections in HEK 293 cells in the presence of synthetic miR-99a, miR-100 or control miRNA precursors. As shown in Figure 3A, the addition of mTOR and IGF-1R 3′ UTR sequences conferred high expression to the luciferase gene, while the raptor 3′ UTR had only a modest effect on luciferase activity. While the expression of all constructs, including the empty vector, was insensitive to the effect of a high concentration (25 nM) of the control miRNA precursor, miR-99a and miR-100 efficiently repressed the expression of luciferase fused to the mTOR and IGF-1R 3′ UTRs in a dose-dependent fashion, starting from a concentration of 5 nM. They also repressed the expression of luciferase-raptor 3′ UTR to baseline levels. Importantly, even the highest concentrations of miR-99a and miR-100 precursors (25 nM) had no effect on the expression of luciferase, indicating that the miRNA effect was specifically mediated by the sequences appended to the 3′ end of the luciferase coding region (Figure 3A). Moreover, IGF-1R, mTOR and raptor 3′ UTRs deleted of their predicted miR-99a/miR-100 binding sites were insensitive to repression by a high concentration (50 nM) of miR-100 precursor that efficiently repressed the wild-type constructs (Figure 3B).

The phosphorylated, active form of the mTOR kinase (p-Ser2448) is specifically enriched in mitotic tumor adrenocortical cells

Considering the potential effect of miRNAs of the miR-100 family in modulating the expression of proteins involved in mTOR signalling, we explored the role of this pathway in regulating the proliferation of adrenocortical tumor cells. We started by studying the cellular localization of mTOR and its Ser2448-phosphorylated, active form. While mTOR is distributed in the cytoplasm of adrenocortical tumor H295R cells, phospho-mTOR is strikingly enriched in mitotic cells (Supplementary Figure 4). In prophase, a bright phospho-mTOR staining appeared among condensed chromosomes, which at metaphase partly colocalized with the mitotic spindle, being also present in a bright dot-like pattern in the cytoplasm of mitotic cells (Figure 4). Starting from anaphase, the phospho-mTOR signal moved to the midzone and progressively concentrated at the midbody in the cleavage furrow during telophase and cytokinesis (Figure 4).

Blockage of mTOR activity inhibits adrenocortical tumor cell proliferation in vitro and xenograft growth

Because of the effects of mTOR signalling on cell growth and proliferation, mTOR inhibitors derived from the macrolide rapamycin are being used in the chemotherapy of different types of cancer (16). Since mTOR signalling is activated in ACT, we studied the effect of the mTOR inhibitor RAD001 (everolimus) on the proliferation of adrenocortical tumor cells H295R and SW-13. The drug significantly inhibited proliferation of both cell lines, showing a more potent effect on SW-13 than on H295R cells (IC_{50} $10^{-8.9}$ M *vs.* $10^{-8.1}$ M; Figure 5A). RAD001 also inhibited the proliferation of primary childhood ACT cells (14), with an IC_{50} of $10^{-9.2}$ M, and of the HAC15 cell line, derived from a pediatric adrenocortical carcinoma (17), with an of IC_{50} $10^{-8.6}$ M (Figure 5A).

We then measured the capacity of RAD001 to inhibit the growth of H295R cells injected as xenografts into NOD/SCID mice. The drug (10 mg/kg/day) significantly inhibited xenograft growth compared to placebo treatment, without inducing detectable side effects on mice (Figure 5B). A lower RAD001 dose (3 mg/kg/day) was not active (data not shown). Tumor weight and the number of mitoses per high-power microscopic field were also significantly lower in RAD001 – treated animals (Supplementary Figure 5A and B). As expected, RAD001 treatment potently reduced phospho-RPS6 expression in the xenografts and also reduced blood vessel number and extension (Supplementary Figure 5C). In addition, we could detect

thrombogenesis in tumor vasculature (Supplementary Figure 5C), as described previously in other animal tumor models (18).

Discussion

Here we have shown that the expression of a distinct set of miRNAs is differentially regulated in childhood ACT, compared to normal adrenal. Interestingly, unsupervised clustering revealed that miRNA profiles could distinguish between two groups of ACT in our series, one of which (T1 in Figure 1) was associated with the risk of relapse. These data need to be validated on a larger series of cases. Consistently with previous results in other types of cancer (19), the majority of the differentially expressed miRNAs in ACT was downregulated compared to normal adrenal. Conversely, one miRNA that was found to be highly upregulated in ACT was miR-483-3p. The gene encoding this miRNA lies within an intron of the *IGF-2* gene in 11p15, which is overexpressed at high frequency in childhood ACT (4,5). Further studies are required to assess the potential role of miR-483-3p overexpression in ACT pathogenesis. Three among the differentially expressed miRs (miR-503, miR-214 and miR-375) were also identified in a study of the miRNA expression profiles in adult ACT, with miR-503 and miR-375 displaying a significantly different expression in carcinomas compared to functioning adenomas (20). Moreover, another recent study described downregulation of miR-195 (which is also downregulated in ACT in our series) and upregulation of miR-483-5p (which is derived from the same precursor as miR-483-3p) as potential prognostic markers in adult ACT (21).

We focused our functional analysis on miR-99a and miR-100, which are among the most highly downregulated miRNAs in ACT. They share the same seed sequence, which suggests that they can regulate a common set of target mRNAs. Here we show that in adrenocortical tumor cells these miRNAs regulate IGF-R and mTOR signalling cascades at multiple levels through modulation of the expression of key proteins implicated in those pathways (Figure 6). Previous reports have shown the importance of the IGF – IGF-R pathway in the regulation of adrenocortical cancer cell proliferation and the efficacy of targeting this pathway in preclinical models of the disease (6,7,15). Here we have shown that IGF-1R levels are upregulated in ACT and that miR-99a/miR-100 can regulate its expression acting on a target site in the 3′ UTR of its mRNA. These data are consistent with previous findings showing overexpression of IGF-1R mRNA in ACT (6). In these tumors, very high IGF-2 mRNA expression often does not translate into the production of a biologically active protein (10). High IGF-1R expression is then likely to play a pivotal role in the activation of the IGF pathway in these tumors.

Studies analyzing other types of tumors revealed that miR-99a and/or miR-100 are also significantly downregulated in ovarian and prostate cancer and in head and neck carcinomas (22-28). Also, the gene encoding miR-99a lies in a region in chromosome 21q21 harboring a putative tumor suppressor gene in lung cancer (29). It is then tempting to speculate that those miRNAs play a role in the modulation of IGF – mTOR signalling also in other types of tumors.

mTOR signalling is closely interconnected with the IGF pathway since it can be activated by upstream IGF receptor signalling. mTOR activity has an essential role in the regulation of various essential cellular processes (30,31). The protein kinase mTOR (FRAP1) has been identified as a target for rapamycin bound to FKBP12. It exists in the cell in two distinct complexes, mTORC1 and mTORC2. The two complexes have different downstream effectors and only mTORC1 is directly sensitive to rapamycin inhibition. Nevertheless, it is known that in some cell lines prolonged treatment with rapamycin also perturbs mTORC2 assembly and inhibits Akt activity (32). The relationship between the mTOR pathway and cancer is complex, since, depending on the cellular context, rapamycin treatment may either inhibit cell growth or activate the oncogenic Akt kinase (33,34). In any case, mTOR inhibition appears particularly promising as a therapeutic tool for cancers characterized by an activated Akt pathway and a

relevant angiogenic component, like adrenocortical tumors (7,35,36). Our data show that everolimus, a rapamycin analogue, efficiently inhibits adrenocortical tumor cell proliferation *in vitro* and *in vivo*. In the clinical setting, it will be interesting to test the efficacy of treatments combining IGF-1R and mTOR inhibitors for the therapy of advanced adrenocortical cancer.

Here we have shown for the first time that the mTOR and raptor proteins are direct targets for miR-99a/miR-100 inhibition in cancer cells. Interestingly, an inhibitory effect of these miRNAs on mTOR and raptor expression was also shown during cytomegalovirus infection (37). In addition, we have revealed an unexpected mitotic localization of the active phosphorylated mTOR form (Ser2448) in adrenocortical cancer cells. Phospho-mTOR staining starts to be dramatically increased at prophase among condensing chromosomes and transfers at the mitotic spindle during metaphase, being localized at the midbody during telophase and cytokinesis. Recently, a similar pattern of subcellular localization of phospho-mTOR has been described in ovarian granulosa (38) and breast cancer cells (39). These findings suggest that active mTOR signalling may have a previously unrecognized role in the regulation of mitosis and cytokinesis through phosphorylation of still undefined substrates. This hypothesis is supported by the finding that in yeast the TOR protein has been shown to affect microtubule stability and morphology and function of the mitotic spindle (40).

In the adrenal gland, activation of the mTOR pathway has also been described in a particular form of benign adrenocortical neoplasm, primary pigmented nodular adrenocortical disease (PPNAD; 41). Interestingly, a recent analysis of miRNA expression in PPNAD showed that miR-100 is one of the most significantly downregulated miRNAs (42). These data suggest that a link between activated mTOR signalling and miR-100 downregulation may also exist in other types of adrenocortical neoplastic diseases.

Supplementary Material

Refer to Web version on PubMed Central for supplementary material.

Acknowledgments

References

1. Libé R, Fratticci A, Bertherat J. Adrenocortical cancer: pathophysiology and clinical management. Endocr Relat Cancer 2007;14:13–28. [PubMed: 17395972]

2. Michalkiewicz E, Sandrini R, Figueiredo B, et al. Clinical and outcome characteristics of children with adrenocortical tumors. An analysis of 254 cases from the International Pediatric Adrenocortical Tumor Registry. J Clin Oncol 2004;22:838–45. [PubMed: 14990639]

3. Ribeiro RC, Sandrini F, Figueiredo B, et al. An inherited p53 mutation that contributes in a tissue-specific manner to pediatric adrenal cortical carcinoma. Proc Natl Acad Sci USA 2001;98:9330–5. [PubMed: 11481490]

4. Wilkin F, Gagné N, Paquette J, Oligny LL, Deal C. Pediatric adrenocortical tumors: molecular events leading to insulin-like growth factor II gene overexpression. J Clin Endocrin Metab 2000;85:2048–56.

5. Rosati R, Cerrato F, Doghman M, et al. High frequency of loss of heterozygosity at 11p15 and IGF2 overexpression is not associated with clinical outcome in childhood adrenocortical tumors positive for the R337H *TP53* mutation. Cancer Genet Cytogenet 2008;186:19–24. [PubMed: 18786438]

6. Almeida MQ, Fragoso MC, Lotfi CF, et al. Expression of insulin-like growth factor-II and its receptor in pediatric and adult adrenocortical tumors. J Clin Endocrinol Metab 2008;93:3524–31. [PubMed: 18611974]

7. Barlaskar FM, Spalding AC, Heaton JH, et al. Preclinical targeting of the type I insulin-like growth factor receptor in adrenocortical carcinoma. J Clin Endocrinol Metab 2009;94:204–12. [PubMed: 18854392]

8. Doghman M, Karpova T, Rodrigues GA, et al. Increased Steroidogenic Factor-1 dosage triggers adrenocortical cell proliferation and cancer. Mol Endocrinol 2007;21:2968–87. [PubMed: 17761949]

9. Doghman M, Lalli E. A matter of dosage: SF-1 in adrenocortical development and cancer. Ann Endocrinol 2009;70:148–52.

10. West A, Neale GA, Pounds S, et al. Gene expression profiling of childhood adrenocortical tumors. Cancer Res 2007;67:600–8. [PubMed: 17234769]

11. Bartel DP. MicroRNAs: genomics, biogenesis, mechanism, and function. Cell 2004;116:281–97. [PubMed: 14744438]

12. Garzon R, Fabbri M, Cimmino A, Calin GA, Croce CM. MicroRNA expression and function in cancer. Trends Mol Med 2006;12:580–7. [PubMed: 17071139]

13. Calin GA, Sevignani C, Dumitru CD, et al. Human microRNA genes are frequently located at fragile sites and genomic regions involved in cancers. Proc Natl Acad Sci USA 2004;101:2999–3004. [PubMed: 14973191]

14. Doghman M, Arhatte M, Thibout H, et al. Nephroblastoma overexpressed/cysteine-rich protein 61/ connective tissue growth factor/nephroblastoma overexpressed gene-3 (NOV/CCN3), a selective adrenocortical cell proapoptotic factor, is down-regulated in childhood adrenocortical tumors. J Clin Endocrinol Metab 2007;92:3253–60. [PubMed: 17566092]

15. Logié A, Boulle N, Gaston V, et al. Autocrine role of IGF-II in proliferation of human adrenocortical carcinoma NCI H295R cell line. J Mol Endocrinol 1999;23:23–32. [PubMed: 10425444]

16. Guertin DA, Sabatini DM. Defining the role of mTOR in cancer. Cancer Cell 2007;12:9–22. [PubMed: 17613433]

17. Parmar J, Key RE, Rainey WE. Development of an adrenocorticotropin-responsive human adrenocortical carcinoma cell line. J Clin Endocrinol Metab 2008;93:4542–6. [PubMed: 18713819]

18. Guba M, Yezhelyev M, Eichhorn ME, et al. Rapamycin induces tumor-specific thrombosis via tissue factor in the presence of VEGF. Blood 2005;105:4463–9. [PubMed: 15671443]

19. Lu J, Getz G, Miska EA, et al. MicroRNA expression profiles classify human cancers. Nature 2005;435:834–8. [PubMed: 15944708]

20. Tömböl Z, Szabó PM, Molnár V, et al. Integrative molecular bioinformatics study of human adrenocortical tumors: microRNA, tissue-specific target prediction, and pathway analysis. Endocr Relat Cancer 2009;16:895–906. [PubMed: 19546168]

21. Soon PS, Tacon LJ, Gill AJ, et al. miR-195 and miR-483-5p identified as predictors of poor prognosis in adrenocortical cancer. Clin Cancer Res 2009;15:7684–92. [PubMed: 19996210]

22. Iorio MV, Visone R, Di Leva G, et al. MicroRNA signatures in human ovarian cancer. Cancer Res 2007;67:8699–707. [PubMed: 17875710]

23. Yang H, Kong W, He L, et al. MicroRNA expression profiling in human ovarian cancer: miR-214 induces cell survival and cisplatin resistance by targeting PTEN. Cancer Res 2008;68:425–33. [PubMed: 18199536]

24. Nam EJ, Yoon H, Kim SW, et al. MicroRNA expression profiles in serous ovarian carcinoma. Clin Cancer Res 2008;14:2690–5. [PubMed: 18451233]

25. Porkka KP, Pfeiffer MJ, Waltering KK, Vessella RL, Tammela TL, Visakorpi T. MicroRNA expression profiling in prostate cancer. Cancer Res 2007;67:6130–5. [PubMed: 17616669]

26. Tran N, McLean T, Zhang X, et al. MicroRNA expression profiles in head and neck cancer cell lines. Biochem Biophys Res Commun 2007;358:12–7. [PubMed: 17475218]

27. Wong TS, Liu XB, Wong BY, Ng RW, Yuen AP, Wei WI. Mature miR-184 as potential oncogenic microRNA of squamous cell carcinoma of tongue. Clin Cancer Res 2008;14:2588–92. [PubMed: 18451220]

28. Henson BJ, Bhattacharjee S, O'Dee DM, Feingold E, Gollin SM. Decreased expression of miR-125b and miR-100 in oral cancer cells contributes to malignancy. Genes Chrom Cancer 2009;48:569–82. [PubMed: 19396866]

29. Yamada H, Yanagisawa K, Tokumaru S, et al. Detailed characterization of a homozygously deleted region corresponding to a candidate tumor suppressor locus at 21q11-21 in human lung cancer. Genes Chrom Cancer 2008;47:810–8. [PubMed: 18523997]

30. Hay N, Sonenberg N. Upstream and downstream of mTOR. Genes Dev 2004;18:1926–45. [PubMed: 15314020]

31. Sarbassov DD, Ali SM, Sabatini DM. Growing roles for the mTOR pathway. Curr Opin Cell Biol 2005;17:596–603. [PubMed: 16226444]

32. Frias MA, Thoreen CC, Jaffe JD, et al. mSin1 is necessary for Akt/PKB phosphorylation, and its isoforms define three distinct mTORC2s. Curr Biol 2006;16:1865–70. [PubMed: 16919458]

33. O'Reilly KE, Rojo F, She QB, et al. mTOR inhibition induces upstream receptor tyrosine kinase signaling and activates Akt. Cancer Res 2006;66:1500–8. [PubMed: 16452206]

34. Sabatini DM. mTOR and cancer: insights into a complex relationship. Nat Rev Cancer 2006;6:729–34. [PubMed: 16915295]

35. Fassnacht M, Weismann D, Ebert S, et al. AKT is highly phosphorylated in pheochromocytomas but not in benign adrenocortical tumors. J Clin Endocrinol Metab 2005;90:4366–70. [PubMed: 15855265]

36. de Fraipont F, El Atifi M, Gicquel C, Bertagna X, Chambaz EM, Feige JJ. Expression of the angiogenesis markers vascular endothelial growth factor-A, thrombospondin-1, and platelet-derived endothelial cell growth factor in human sporadic adrenocortical tumors: correlation with genotypic alterations. J Clin Endocrinol Metab 2000;85:4734–41. [PubMed: 11134136]

37. Wang FZ, Weber F, Croce C, Liu CG, Liao X, Pellett PE. Human cytomegalovirus infection alters the expression of cellular microRNA species that affect its replication. J Virol 2008;82:9065–74. [PubMed: 18596100]

38. Yaba A, Bianchi V, Borini A, Johnson J. A putative mitotic checkpoint dependent on mTOR function controls cell proliferation and survival in ovarian granulosa cells. Reprod Sci 2008;15:128–38. [PubMed: 18276949]

39. Vazquez-Martin A, Oliveras-Ferraros C, Bernadó L, López-Bonet E, Menendez JA. The serine 2481-autophosphorylated form of mammalian Target Of Rapamycin (mTOR) is localized to midzone and midbody in dividing cancer cells. Biochem Biophys Res Commun 2009;380:638–43. [PubMed: 19285014]

40. Choi JH, Adames NR, Chan TF, Zeng C, Cooper JA, Zheng XF. TOR signaling regulates microtubule structure and function. Curr Biol 2000;10:861–4. [PubMed: 10899009]

41. Mavrakis M, Lippincott-Schwartz J, Stratakis CA, Bossis I. Depletion of type IA regulatory subunit (RIα) of protein kinase A (PKA) in mammalian cells and tissues activates mTOR and causes autophagic deficiency. Hum Mol Genet 2006;15:2962–71. [PubMed: 16963469]

42. Iliopoulos D, Bimpaki EI, Nesterova M, Stratakis CA. MicroRNA signature of primary pigmented nodular adrenocortical disease: clinical correlations and regulation of *Wnt* signaling. Cancer Res 2009;69:3278–82. [PubMed: 19351815]
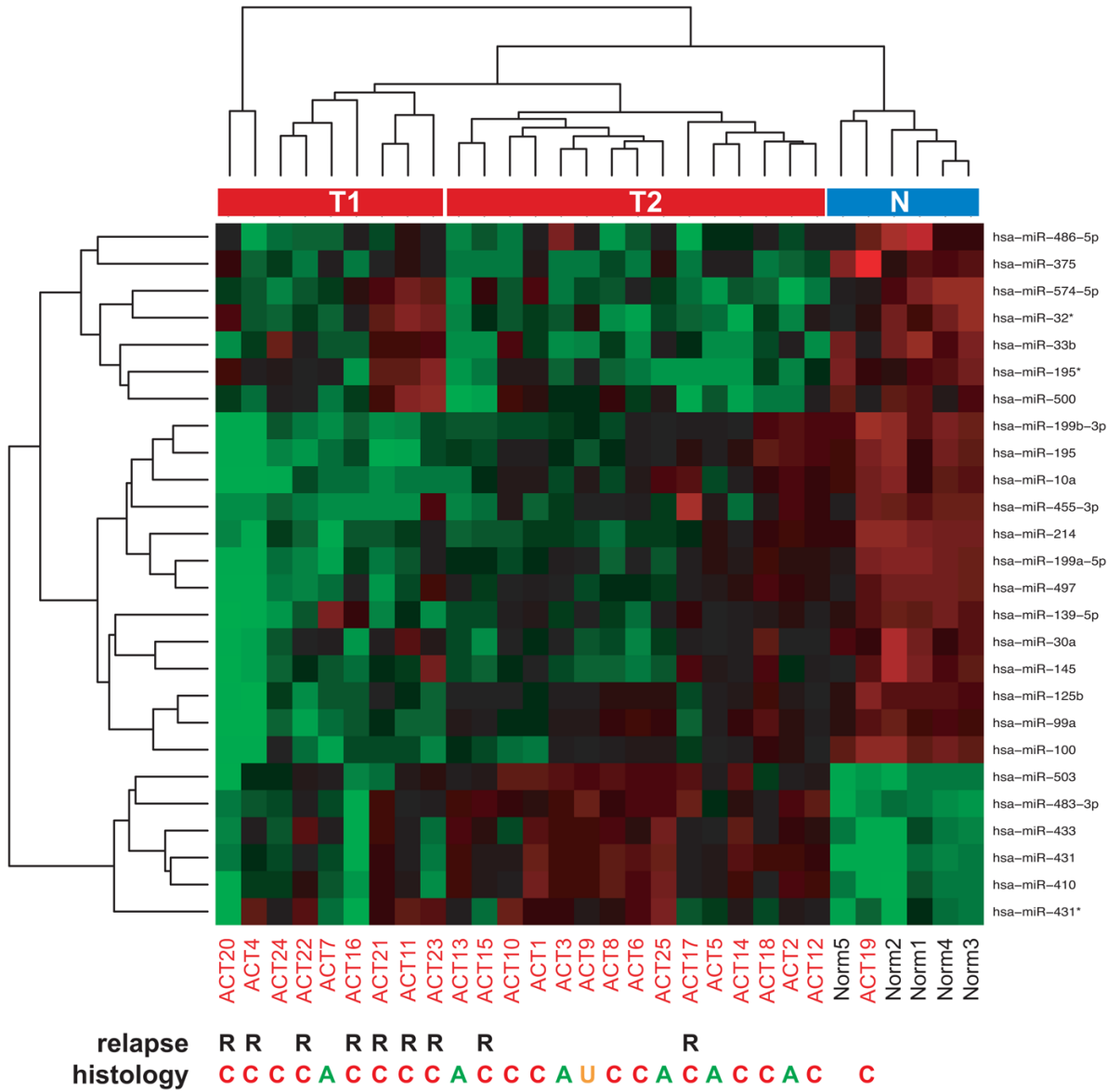
Figure 1. Identification of differentially expressed miRNAs in childhood ACT
Heatmap plot of significantly differentially expressed miRNAs in childhood ACT compared to normal adrenal cortex. R, indicates patients with relapse. A, adenoma (Weiss index <3); C, carcinoma (Weiss index ≥3); U, unknown histological type. Unsupervised clustering divides tumor miRNA expression profiles into two distinct groups (T1 and T2). N, normal adrenal cluster.
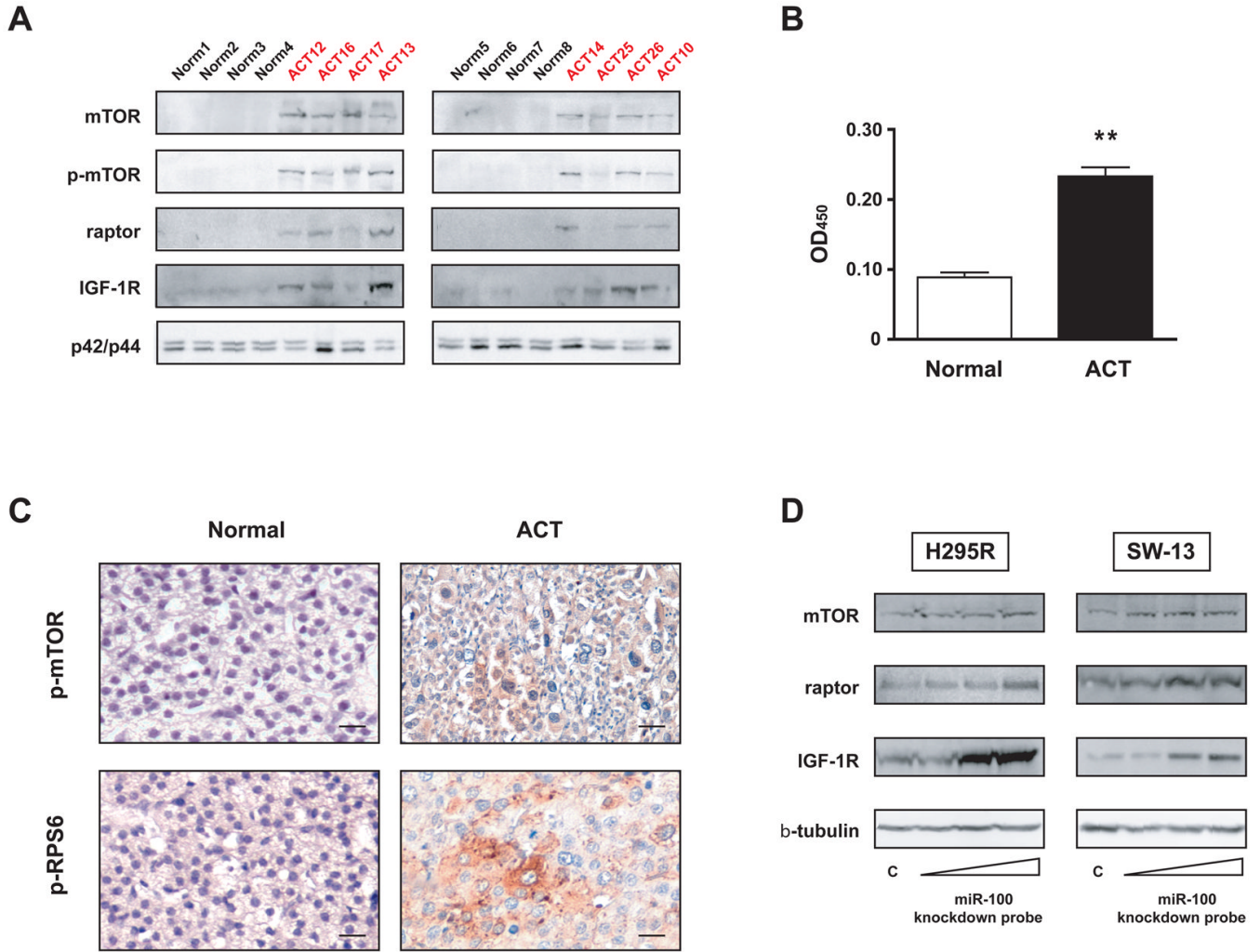
Figure 2. mTOR signalling is activated in childhood ACT and knockdown of endogenous miR-100 regulates expression of mTOR, raptor and IGF-1R proteins in adrenocortical tumor cells
A, Immunoblot showing expression of mTOR, phospho-mTOR (Ser 2448), raptor and IGF-1R proteins in a series of 8 ACTs (ACT10, 12, 13, 14, 16, 17, 25, 26; see Supplementary Table 1 for patients' clinical data) and 8 normal adrenal cortex samples. p42/p44 expression is shown as loading control. Quantification of immunoblot results is shown in Supplementary Figure 3. *B*, mTOR kinase activity against recombinant GST-p70S6K was measured in 8 ACTs (ACT7, 9, 11, 15, 16, 27, 28, 29; see Supplementary Table 1 for clinical data) and 3 normal adrenal cortex samples by EIA. ** $p<0.01$, Student's *t*-test. *C*, Top, immunohistochemistry showing strong diffuse expression of phospho-mTOR (Ser 2448) in one ACT sample (ACT30; see Supplementary Table 1 for patients' clinical data). Bottom, focal phospho-RPS6 (Ser240/244) staining in another ACT sample (ACT 32). 40X magnification, bar = 20 μm in all panels. Quantification of IHC results for each patient analyzed is shown in Supplementary Table 3. *D*, H295R (left) and SW-13 (left) tumor adrenocortical cells were transfected with increasing concentrations (10, 25 and 50 nM) of miR-100 knockdown probe or scramble control (50 nM). Expression of endogenous mTOR, raptor and IGF-1R proteins was revealed by immunoblot 48 hours after transfection. β-tubulin expression is shown as loading control.

A

B
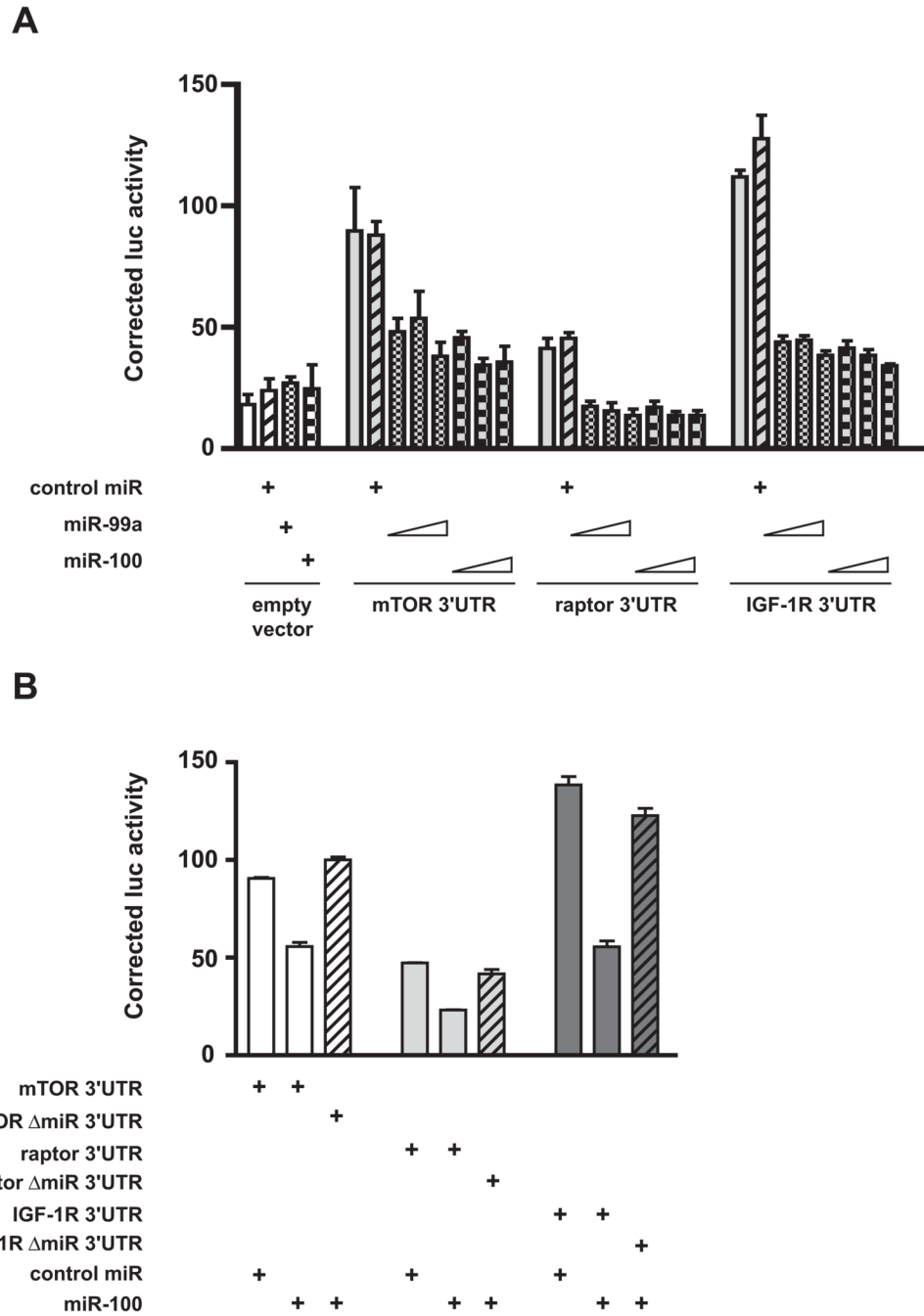
Figure 3. Regulation of mTOR, raptor and IGF-1R expression by miR99a/miR-100 through their 3′ UTRs

A, Increasing concentrations of miR-99a and miR-100 pre-miRs (5, 10 and 25 nM) repress expression of *Renilla* luciferase harboring mTOR, raptor and IGF-1R 3′ UTR sequences in transfected HEK 293T cells. No significant effect was detected for 25 nM control pre-miR. The weak activity of the transfected empty vector (psiCHECK-2) was not affected by cotransfection with any of the pre-miRs. *B*, Pre-miR-100 (50 nM) efficiently represses activity of luciferase – mTOR, – raptor and – IGF-1R 3′ UTRs, while constructs with deleted miRNA binding sites for each 3′ UTR are not sensitive to repression by pre-miR-100.
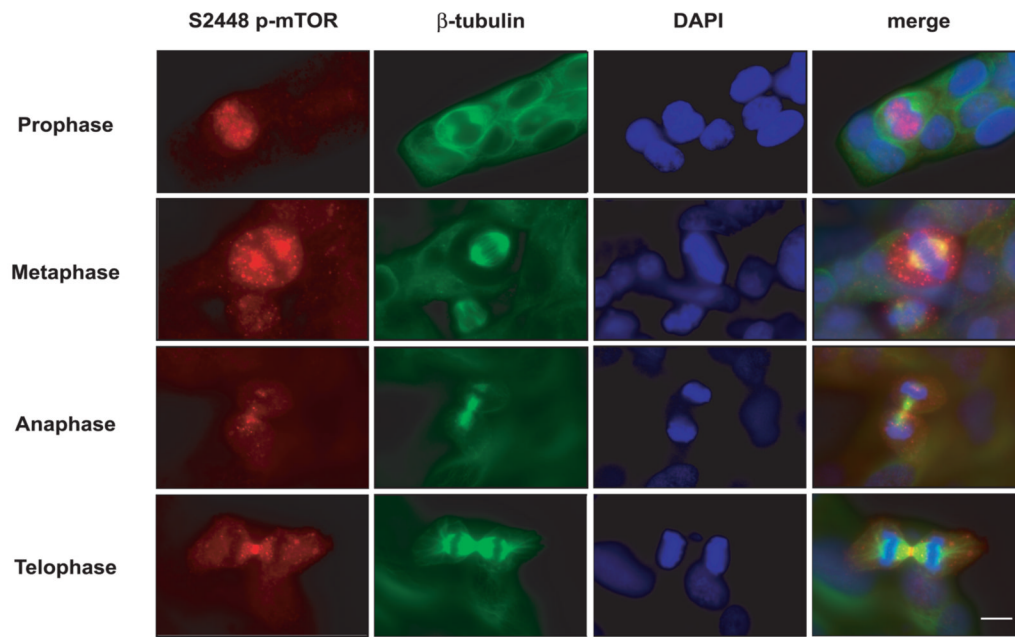
Figure 4. Phospho-mTOR (Ser 2448) is specifically expressed during mitosis in human adrenocortical tumor cells
The expression of phospho-mTOR (Ser2448) (in red) was revealed by immunofluorescence during the different stages of mitosis in H295R cells. β-tubulin expression is shown in green and DAPI staining in blue. 100x magnification, bar = 10μm.

A

B
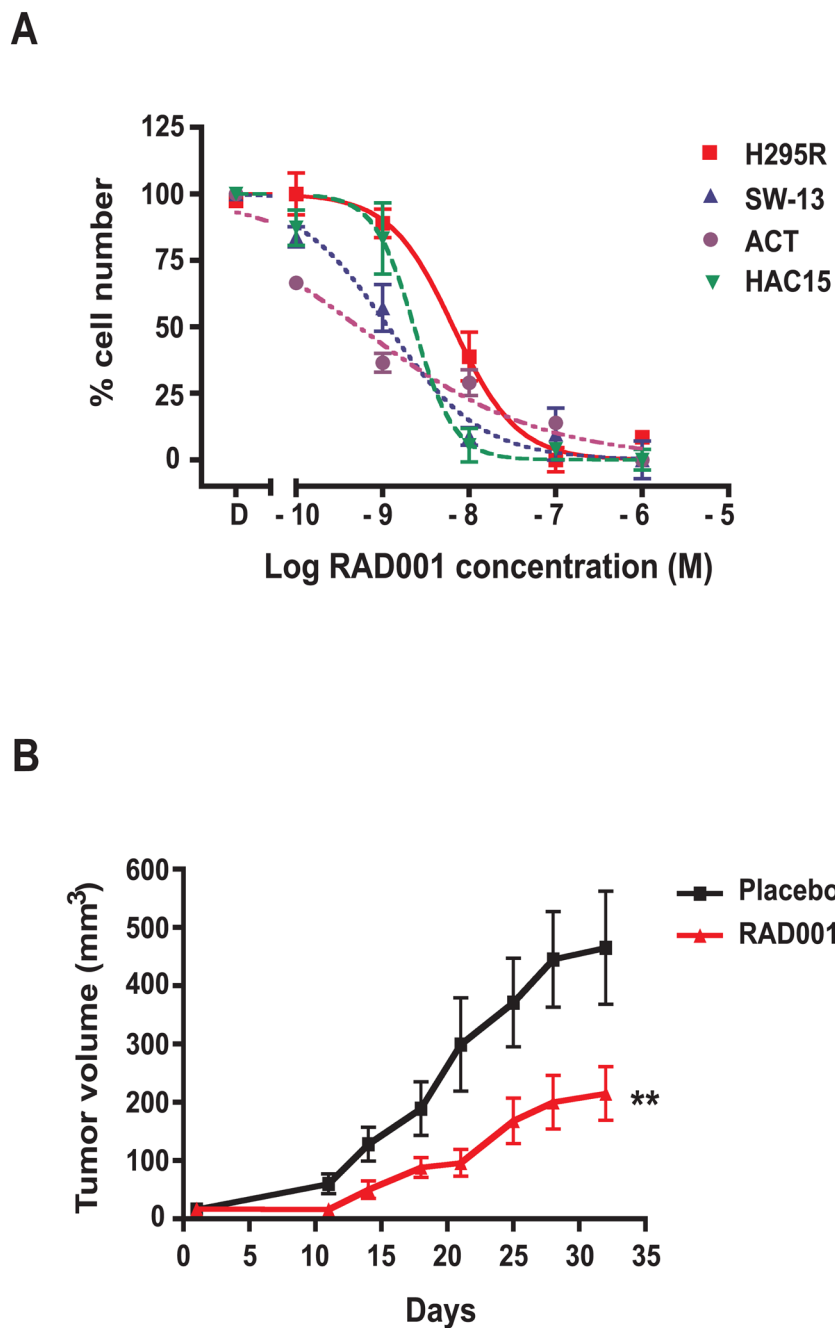
Figure 5. The rapamycin analogue RAD001 inhibits adrenocortical tumor cell growth *in vitro* and *in vivo*

A, H295R (red squares), SW-13 (blue triangles), primary ACT (purple circles) and HAC15 (green triangles) cells were cultured in 24-well plates in the presence of DMSO (D) or of increasing concentrations of RAD001. Cells were counted after 6 days of culture in the presence of the drug. SEM is indicated. Data were generated from three different experiments each performed in duplicate. *B*, H295R xenograft growth in NOD/SCID/γ_c^{null} mice treated with placebo (black squares) or with RAD001 (10/mg/kg/day; red triangles). SEM is indicated. Tumor growth was significantly different (**$p<0.01$, paired *t*-test) in animals treated with the drug.
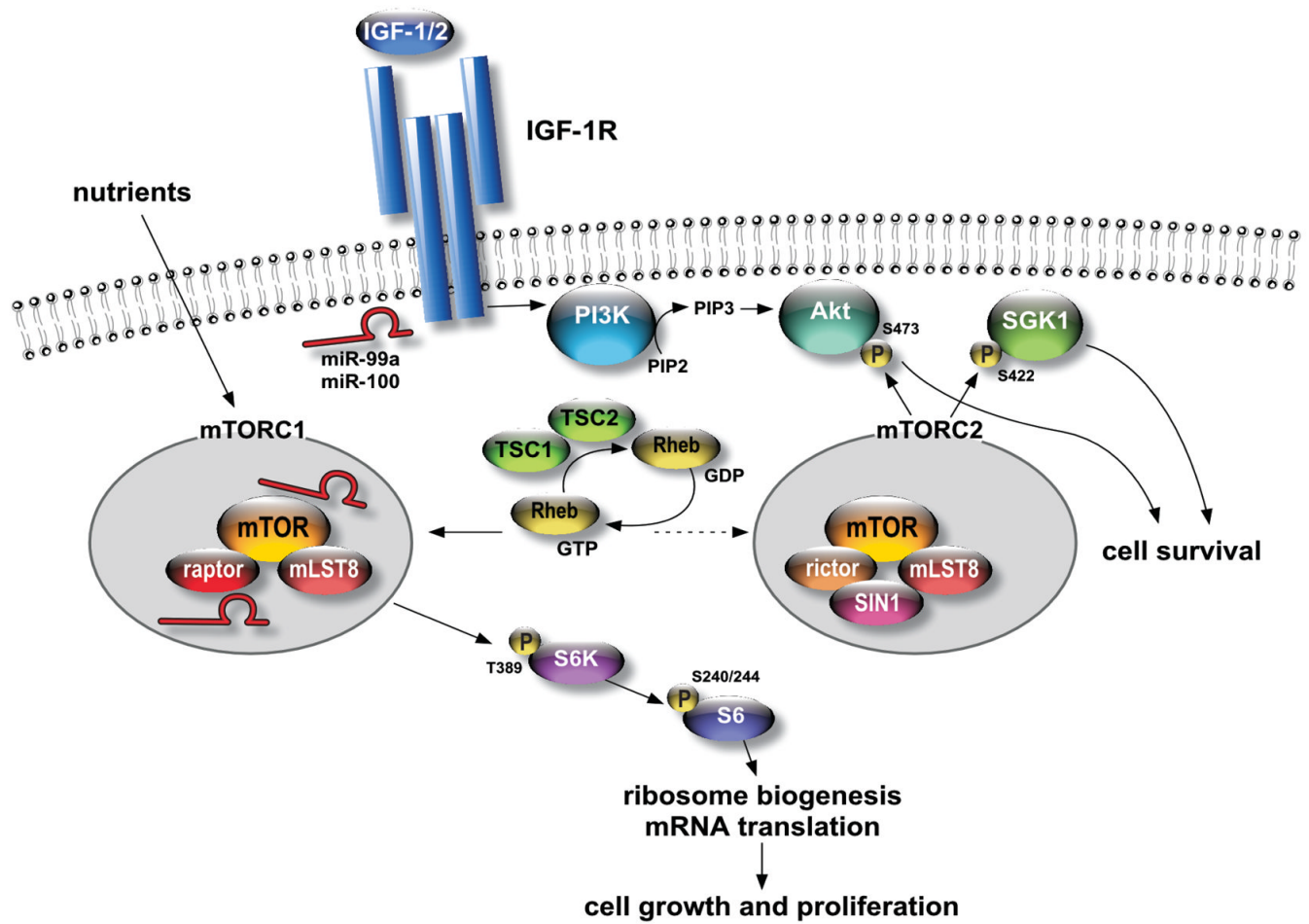
Figure 6. miR-99a/miR-100 regulate IGF – mTOR signalling at multiple levels
A simplified view of IGF – mTOR signalling. Key targets of miR-99a/miR-100 (indicated in red) regulation are indicated.